ISSN 1674-1056
http://cpb.iphy.ac.cn
http://iopscience.iop.org/cpb
中国物理 B
Chinese Physics
中国物理 Chinese Physics B

Collision of cold CaF molecules: Towards evaporative cooling

Yuefeng Gu(顾跃凤), Yunxia Huang(黄云霞), Chuanliang Li(李传亮), Xiaohua Yang(杨晓华)

Citation: Chin. Phys. B . 2019, 28(3): 033401. **doi:** 10.1088/1674-1056/28/3/033401
Journal homepage: http://cpb.iphy.ac.cn; http://iopscience.iop.org/cpb

What follows is a list of articles you may be interested in

Solvent effects and potential of mean force study of the S_N2 reaction of CH_3F+CN^- in water

Chen Li(李琛), Peng Liu(刘鹏), Yongfang Li(李永方), Dunyou Wang(王敦友)

Chin. Phys. B . 2018, 27(3): 033401. **doi:** 10.1088/1674-1056/27/3/033401

Combined multi-level quantum mechanics theories and molecular mechanics study of water-induced transition state of OH^-+CO_2 reaction in aqueous solution

Chen Li(李琛), Meixing Niu(牛美兴), Peng Liu(刘鹏), Yongfang Li(李永方), Dunyou Wang(王敦友)

Chin. Phys. B . 2017, 26(10): 103401. **doi:** 10.1088/1674-1056/26/10/103401

Intrinsic product polarization and branch ratio in the$S(^1D, ^3P)+HD$ reaction on three electronic states

Lin Li(李琳), Shunle Dong(董顺乐)

Chin. Phys. B . 2016, 25(9): 093401. **doi:** 10.1088/1674-1056/25/9/093401

The influence of 3d-metal alloy additions on the elastic and thermodynamic properties of $CuPd_3$

Huang Shuo, Zhang Chuan-Hui, Sun Jing, Shen Jiang

Chin. Phys. B . 2013, 22(8): 083401. **doi:** 10.1088/1674-1056/22/8/083401

Chen's lattice inversion embedded-atom method for Ni–Al alloy

Zhang Chuan-Hui, Huang Shuo, Shen Jiang, Chen Nan-Xian

Chin. Phys. B . 2012, 21(11): 113401. **doi:** 10.1088/1674-1056/21/11/113401

Collision of cold CaF molecules: Towards evaporative cooling*

Yuefeng Gu(顾跃凤)[1], Yunxia Huang(黄云霞)[1], Chuanliang Li(李传亮)[2], and Xiaohua Yang(杨晓华)[1,3,†]

[1] *School of Science, Nantong University, Nantong* 226019, *China*
[2] *Department of Physics, School of Applied Science, Taiyuan University of Science and Technology, Taiyuan* 030024, *China*
[3] *State Key Laboratory of Precision Spectroscopy, East China Normal University, Shanghai* 200062, *China*

(Received 14 November 2018; revised manuscript received 18 December 2018; published online 23 January 2019)

Long range intermolecular interaction potential surface of CaF ($^2\Sigma^+$) was simulated by employing the MOLPRO program and using the RCCSD(T)/def2-TZVP theory. The predicted data were further fitted to obtain the collision cross-section. The elastic collision cross-section of CaF at the temperature around 2 mK is as high as 6.5×10^{-9} cm^2 and the collision rate is over 4.1×10^6 Hz. Additionally, we found that an orientation electric field will simplify the intermolecular interaction potential function from quaternary into ternary and the collision cross-section will be raised by about three orders. All-optical evaporative cooling of cold CaF is discussed in the conclusion.

Keywords: intermolecular interaction potential energy surface, cold collision, evaporative cooling

PACS: 34.20.–b, 37.10.Mn **DOI:** 10.1088/1674-1056/28/3/033401

1. Introduction

Cold molecular collision is one of the important aspects in the study of cold molecules. Quantum effects become important and even dominate the cold collision at low temperatures, where few partial waves contribute and the de Broglie wavelength associated with the relative velocity becomes comparable to or larger than the intermolecular distances.[1] Owing to the rapid progresses in the field of cold molecules in the past two decades, various cold molecules have been achieved experimentally, which has enabled investigations on cold molecular interaction and reaction.[2] Meanwhile, evaporative cooling appears to be the ultimate means to further cool the molecules to the μK region, and even to realize molecular Bose–Einstein condensation or Fermi-degeneracy, which is dominated by the molecular collision.

The calcium monofluoride (CaF) molecule has many potential applications.[3–6] The rovibronic ground state of CaF is high-field-seeking and no Majorana transition allows.[7] Additionally, when the temperature T fulfills $k_{\rm B}T < 2hB$, where $k_{\rm B}$ is the Boltzmann constant, h is the Planck constant, and B is the molecular rotational constant, the inelastic collision is impossible,[8,9] which implies that there is little trapping loss. Thus, CaF is a good candidate for evaporative cooling. However, no molecule–molecule interaction of CaF has been reported so far.

At the RCCSD(T)/default-2 triple-zeta valence polarized (def2-TZVP) level, the interaction potential surface of CaF in the ground state $X^2\Sigma^+$ is fitted in the present work. Furthermore, the simplification of an orientation electrostatic field to the interaction potential is discussed. Our study shows that the collision cross-section will be enhanced significantly by the applied field. Finally, the evaporative cooling of CaF in an all-optical trap is also simulated.

2. Model and theory

Figure 1 shows the molecular coordinates of the two CaF molecules.[10] The z axis originates from the center-of-mass of one molecule (A) and indexes to that of the other (B), $\boldsymbol{R}$ represents the vector of the two center-of-mass from A to B, molecule A locates in the plane of xOz, θ_A and θ_B are the angles between the molecular axis (the direction is from atom Ca to F) and $\boldsymbol{R}$ of the two molecules, ϕ is the dihedral angle of the plane of molecule B and z axis with the plane xOz, and $r_{\rm CaF}$ is the length of the molecular bond. The equilibrium nuclear distance of CaF ($X^2\Sigma^+$, $\upsilon = 0$) is 1.967 Å.[11]

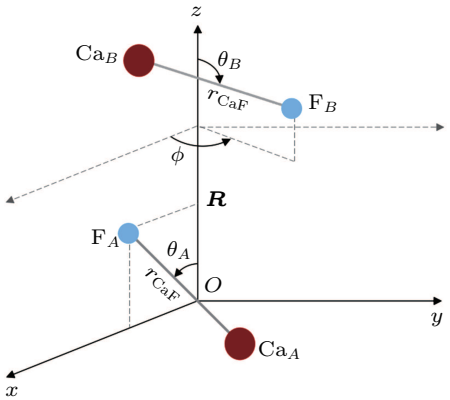


Fig. 1. Molecular coordinates of the CaF–CaF bimolecular system.

*Project supported by the National Natural Science Foundation of China (Grant Nos. 11604164 and U1810129), the Fund for Shanxi "1331 Project" Key Innovation Research Team, China (Grant No. 1331KIRT), and Excellent Youth Academic Leader in Higher Education of Shanxi Province, China (2018).

†Corresponding author. E-mail: xhyang@ntu.edu.cn

© 2019 Chinese Physical Society and IOP Publishing Ltd

CaF is an open shell molecule with electronic spin of 1/2, thus its dimer can either be a singlet ($S=0$) or a triplet ($S=1$). Therefore, the intermolecular interaction potential is determined by[10]

$$\overline{V}(R,\theta_A,\theta_B,\phi) = \frac{3}{4}V^{S=1}(R,\theta_A,\theta_B,\phi) + \frac{1}{4}V^{S=0}(R,\theta_A,\theta_B,\phi). \quad (1)$$

Equation (1) can be computed using MOLPRO program[12] with the counterpoise correction method of Boys and Bernardi,[10,13]

$$V(R,\theta_A,\theta_B,\phi) = E^{\mathrm{DB}}_{\mathrm{dimer}}(R,\theta_A,\theta_B,\phi) - E^{\mathrm{DB}}_{A}(R,\theta_A,\theta_B,\phi) - E^{\mathrm{DB}}_{B}(R,\theta_A,\theta_B,\phi), \quad (2)$$

where the computations of the energies of the single molecules and the dimer are both in the dimer basis (DB), and both atoms of the other CaF are present as ghost atoms when computing the energy of one CaF molecule. In addition, we employed complete active space self-consistent-field (CASSCF) theory[14,15] to calculate the interaction potential $V^{S=0}$ of the singlet state dimer, while we employed the spin-restricted coupled cluster method with single and double excitations and a perturbative treatment of triples [RCCSD(T)],[16] where the basis sets were both def2-TZVP in the series of turbomole def2 and the energy convergence threshold was set to be $10^{-12}E_{\mathrm{h}}$. As stated by Liesbeth *et al.*,[17] in the low temperature and low dense molecular system, the long range potential dominates the molecular dynamics. Thus, only those intermolecular interaction potentials with $R > 10a$, where a is the Bohr radius, were computed in the present work.

The four-dimension potential surface $V(R,\theta_A,\theta_B,\phi)$ in the molecular coordinates can be expanded in terms of spherical harmonics $Y_{L,M}$ of degree L and order M as[10,17–19]

$$V(R,\theta_A,\theta_B,\phi) = \sum_{L_A,L_B,L_{AB}} v_{L_A,L_B,L_{AB}}(R) \times A_{L_A,L_B,L_{AB}}(\theta_A,\theta_B,\phi), \quad (3)$$

where L_{AB} is coupled by L_A and L_B. The angular function $A_{L_A,L_B,L_{AB}}(\theta_A,\theta_B,\phi)$ is defined as follows:

$$\begin{aligned} &A_{L_A,L_B,L_{AB}}(\theta_A,\theta_B,\phi) \\ &= \sum_{M=-\min(L_A,L_B)}^{\min(L_A,L_B)} \begin{pmatrix} L_A & L_B & L_{AB} \\ M & -M & 0 \end{pmatrix} \\ &\times C_{L_A,M}(\theta_A,\phi_A) \times C_{L_B,-M}(\theta_B,\phi_B) \\ &= \sum_{M=0}^{\min(L_A,L_B)} (-1)^M \begin{pmatrix} L_A & L_B & L_{AB} \\ M & -M & 0 \end{pmatrix} A_{L_A,L_B,M}(\theta_A,\theta_B,\phi), \end{aligned} \quad (4)$$

where ϕ_i ($i = A$ or B) are the azimuthal angles of monomers and $\phi = \phi_A - \phi_B$, the symbol $(\cdots)$ is the Wigner-3j symbol, $C_{L,M}(\theta,\phi)$ is the Racah-normalized spherical harmonics, and

$$A_{L_A,L_B,M}(\theta_A,\theta_B,\phi) = P_{L_A,M}(\cos\theta_A) P_{L_B,M}(\cos\theta_B)\cos(M\phi), \quad (5)$$

where $P_{L,M}(\cos\theta)$ is the Schmidt semi-normalized associated Legendre function

$$P_{L,M}(\cos\theta) = \left[(2-\delta_{M,0})\frac{(L-M)!}{(L+M)!}\right]^{1/2} (1-\cos^2\theta)^{M/2} \times \frac{\mathrm{d}^M}{\mathrm{d}(\cos\theta)^M} P_L(\cos\theta), \quad (6)$$

where $P_L(\cos\theta)$ is the Legendre polynomials. In addition, in the long range interaction approximation, the term $v_{L_A,L_B,L_{AB}}(R)$ in Eq. (3) can be expanded in terms of the power series of $1/R$ as

$$v_{L_A,L_B,L_{AB}}(R) = \sum_n \frac{-C_{L_A,L_B,L_{AB},n}}{R^n}. \quad (7)$$

Therefore, the ground state CaF intermolecular long range interaction potential was computed, and thus the four-dimensional potential surface was numerically fitted in the present work. To compare with the literature,[10,17] when we computed the potential $V(R,\theta_A,\theta_B,\phi)$, the variables were set as follows: R was set to 30 different values varying from $12a$ to $2000a$; θ_i were set to different values varying from 0° to 180° with the step of 20° and an additional 90°; ϕ was set to different values varying from 0° to 180° with the step of 22.5°; and in the fitting process of potential, $L_i \leq 10$ and $n \leq 14$ in Eq. (7).

3. Results and discussion

3.1. Collision in the field-free case

Before computing the four-dimensional potential surface, we studied the CaF intermolecular interaction potential difference under the singlet and triplet systems. We computed the potential varying with the intermolecular distance with 27 sets of azimuthal angles. Some of these results are plotted in Fig. 2, where the red lines represent the weighted average potentials according Eq. (1). As evidenced in Fig. 2, the average potentials approach to those of the triplet in the long range ($> 60a$) region, despite their large differences in the short range region. Meanwhile, the densest cold CaF molecules cloud achieved in the recent experiment had a density of 8(2) $\times 10^7$ cm^{-3},[6] where the intermolecular mean distance is at the order of $2 \times 10^5 a$, and thus CaF can hardly pair to form the singlet dimer at the typical experimental condition. Therefore, to lower the computation cost, we computed the four-dimension potential surface at the triplet dimer approximation.

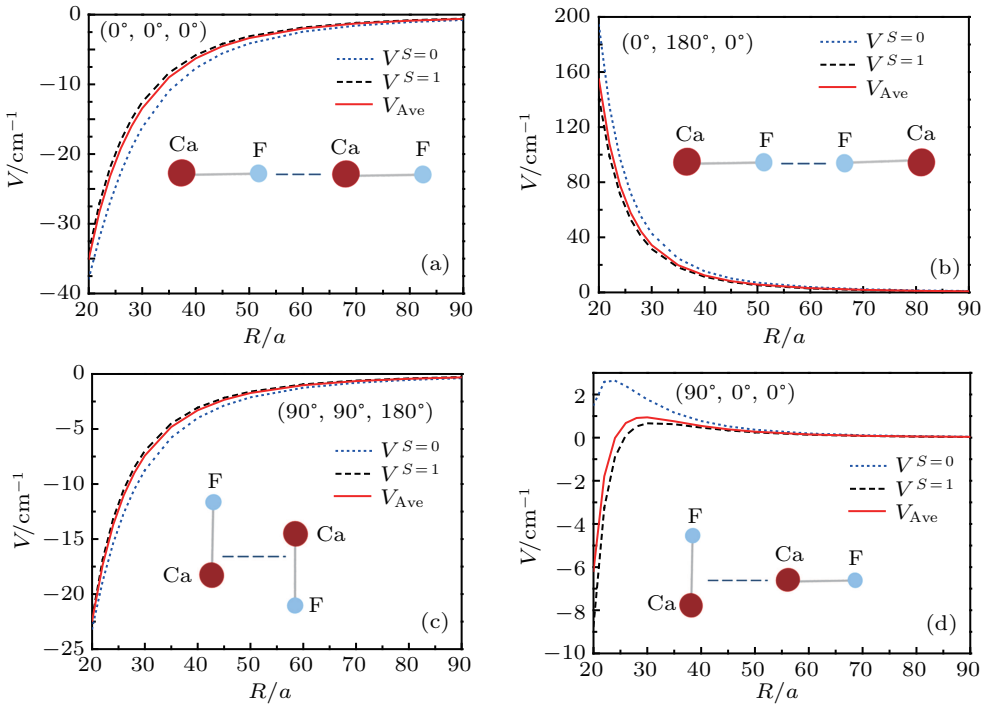


Fig. 2. Molecular interaction potentials of $V^{S=0}$ (dot), $V^{S=1}$ (dash) and weighted average ones (solid) as functions of the molecular distance at (a)–(d) different azimuthal angles $(\theta_A, \theta_B, \phi)$, and the insets show the molecular location relations of the two molecules.

We computed 32670 potential points employing MOLPRO program to obtain high precision potential surface $V^{S=1}(R, \theta_A, \theta_B, \phi)$, and fitted to achieve 506 sets of $v_{L_A,L_B,L_{AB}}(R)$. Some of the high order items, when $L_i = 10$ and $L > 10$, appeared to be zero arose from the large separation azimuthal angles we set. If necessary, the high precision, high order items could also be determined. The obtained numerical potential points were non-linear least-squares fitted using Eq. (7) to obtain $v_{L_A,L_B,L_{AB}}(R)$, as shown in Fig. 3, which implies the precision of our results.

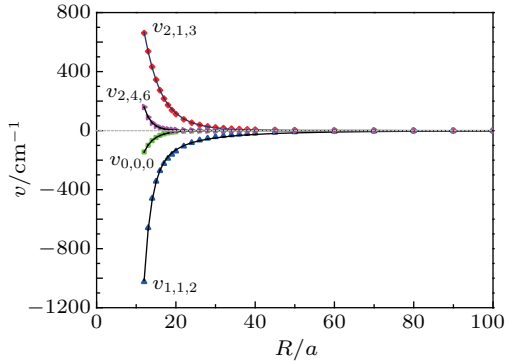


Fig. 3. Partial of the non-linear least-squares fitted results of $v_{L_A,L_B,L_{AB}}(R)$, where the dots were simulated and the lines were fitted.

Different kinds of intermolecular interactions do not contribute equally to the collision cross-section. One has to determine the domination to estimate the cross-section. Liesbeth *et al.*[17] determined that the contribution of each coefficient to the interaction potential at the long range region can be expressed as

$$V_{L_A,L_B,L_{AB},n}(R) = \sqrt{\frac{4\pi}{(2L_A+1)(2L_B+1)(2L_{AB}+1)}} \times \frac{|C_{L_A,L_B,L_{AB},n}|}{R^n}. \quad (8)$$

As to polar CaF, the dipole–dipole and dipole–quadrupole interactions contribute most to the electrostatic multipole–multipole interaction (first-order contributions) and the dipole-induced-dipole interaction contributes most to the polarized interaction (second-order contributions). Figure 4 presents the potentials $V_{1,1,2,3}$, $V_{1,2,3,4}$, and $V_{0,0,0,6}$ versus the intermolecular distance to visually show their contributions. This shows that the dipole–dipole interaction dominates the potential, especially in the long range region. Therefore, other interactions can be treated as perturbations to the dipole–dipole one, and can be neglected in the typical experimental condition at present.

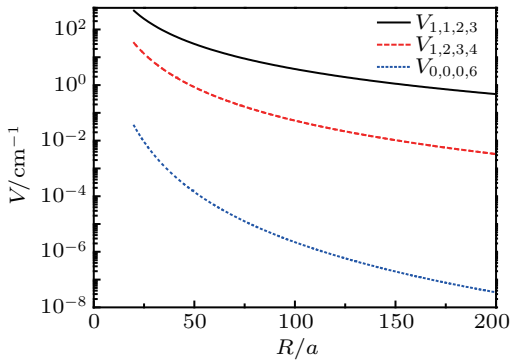


Fig. 4. The dipole–dipole ($V_{1,1,2,3}$), dipole–quadrupole ($V_{1,2,3,4}$), and dipole-induced-dipole ($V_{0,0,0,6}$) interactions of CaF vs. intermolecular separation R.

At the low molecular dense limit, the intermolecular elastic collision cross-section can be simplified as[20] (only considering the dipole–dipole interaction)

$$\sigma_{\mathrm{D-D}} \approx \sqrt{\frac{m\,[\mathrm{a.m.u.}]}{T\,[\mathrm{K}]}}\,\langle \mu\,[\mathrm{D}]\rangle^2 \times 4 \times 10^{-12} \quad [\mathrm{cm}^2]. \qquad (9)$$

The elastic cross-section of the ground state CaF with a permanent dipole $\mu = 3.07$ D[21] at 2 mK is $\sigma_{\mathrm{D-D}} = 6.48 \times 10^{-9}$ cm^2. The cross-section is very large compared with that of other molecules. Thus, its collision rate would be

$$K \approx \sqrt{\frac{8k_{\mathrm{B}}T}{\pi \cdot m}}\rho\sigma_{\mathrm{D-D}} = 4.10 \times 10^6 \quad [\mathrm{Hz}], \qquad (10)$$

with $\rho = 1.78 \times 10^{11}$ cm^{-3} at 2 mK, achieved via two-stage cryogenic buffer gas cooling and laser deceleration[6] and further loaded and compressed in an all-optical three-dimensional trap with the beam waist about 0.10 mm. This collision rate is much larger than that of Ref. [22], which suggests that the evaporative cooling process of CaF molecules would be implemented.

3.2. Collision in an orientation electric field

The investigation of intermolecular interaction is also in favor of cold molecular collision dynamics. The (ultra-)cold collision of CaF is very complex, and the quaternary potential surface function is hard either to analyze or understand, which are challenging to both the investigators and readers. Fortunately, CaF can be readily orientated due to both its relatively large permanent dipole and small rotational constant $B = 0.3385$ cm^{-1}.[23] Figure 5 shows the orientation degree $\langle \cos\theta \rangle$ of CaF in the $|N = 0, M = 0\rangle$ state at the temperature of 1 mK varying with the applied electric field E, where θ is the angle between the molecular dipole and the applied electric field.[24,25] It can be well-oriented (with an orientation degree about 0.9), even at weak field as low as 10 kV/cm, as shown in Fig. 5. Therefore, if CaF molecules are fully orientated—i.e., $\theta = \theta_A = \theta_B$ and $\phi = 0°$—, then the potential surface function will reduce to be ternary. The inset in Fig. 5 shows the intermolecular long range interaction potential surface in the ideal orientation degree of 1, which shows that the largest repulsion potential occurs at $(\theta_A, \theta_B, \phi) = (90°, 90°, 0°)$—i.e., in the shoulder-to-shoulder case—, while the largest attraction potential does not occur at (0°, 0°, 0°) or (180°, 180°, 0°)—i.e., in the head-to-tail case. The simplification of the potential surface would help us to model the cold molecular collision.[26]

However, in a real case, the molecules cannot be fully orientated. We estimated that when the orientation degree is 0.96 obtained at the applied field of 100 kV/cm, only about 6% error of the cross-section arises. Therefore, in the high orientation case, the potential surface can be approximately determined using the simplified ternary model.

Additionally, the applied field to orientate the molecules will raise the intermolecular collision cross-section due to the field-induced molecular dipole, which depends on the polarizability. The polarizability tensor was calculated using the CCSD(T) theory on the basis of turbomole def2 series sets employing ORCA program,[27] and is listed in Table 1. In the homogeneous applied field along the z axis, the component α_{zz} means and the total dipoles in the applied field were calculated. Judging from the obtained dipole, the polarizability $\alpha_{zz} = 101.533567$ a.u. would be the most confident one obtained at CCSD(T)/def2-QZVP set.

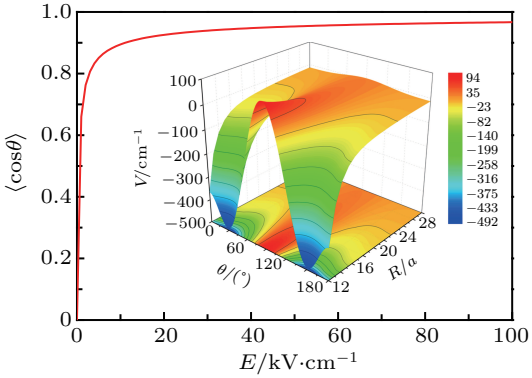


Fig. 5. Molecular orientation depth $\langle \cos\theta \rangle$ of the $|N = 0, M = 0\rangle$ state of CaF varying with applied electrostatic field E. The inset shows the intermolecular interaction potential surface at long range interaction region at the fully oriented approximation (the orientation depth equals 1).

Table 1. Calculated component α_{zz} of the polarizabilty tensor and molecular dipole μ at the CCSD(T) level in the basis of turbomole def2 series at different basis sets.

Basis set	α_{zz}/a.u.	μ/D
def2-SVP	58.51194	3.52419
def2-SVPD	96.54192	3.06298
def2-TZVP	92.50011	3.17505
def2-TZVPD	97.30601	3.11859
def2-QZVP	101.53567	3.07338
def2-QZVPD	102.03072	3.08193

The induced dipole is 5.0×10^{-3} D at the applied field of 100 kV/cm. Figure 6 presents, in the dipole–dipole interaction approximation, the elastic collision cross-section σ at the applied field of 100 kV/cm and its increment $\Delta\sigma$ compared to field-free one σ varying with the molecular temperature at the order of several mK. That the relative increment of collision cross-section $\Delta\sigma/\sigma \approx 3 \times 10^{-3}$ indicates that the applied field contributes little to the evaporative cooling in this temperature region.

However, the dipole-induced-dipole interaction increases gradually with the decrease of the intermolecular distance—it would even overtake the dipole–dipole interaction, as shown in Fig. 4. Actually, the dipole-induced-dipole interaction dominates the collision of the high dense ultracold (below 1 mK)

molecules. Kajita pointed out that the electric dipole–dipole interaction is only significant for the collision between the same ultracold fermionic molecules, and he gave the equation of the elastic collision cross-section of the ultracold bosonic molecules when only the dipole-induced-dipole interaction is included,[9]

$$\sigma_{\mathrm{D-ID}} = \frac{2\pi}{k^2} \sum_{L,M_L} P(L,M_L), \tag{11}$$

where matter wave vector $k = (2mE_{\mathrm{ck}}/\hbar^2)^{1/2}$ (here m is the mass of the molecule and E_{ck} is the collision kinetic energy), L is the quantum number of the relative motion, M_L is its trajectory parallel to the external field, and P denotes the probability of the scattering of each partial wave. Meanwhile, Kajita concluded that the elastic collision cross-section approaches to an appreciable value as the temperature of the ultracold boson molecules reaches the order of mK. For CaF molecules at 1 μK, its collision cross-section $\sigma_{\mathrm{D-ID}} = 5.897 \times 10^{-12}$ cm^2 is about one order larger than that of ^{15}NH if only the s-wave scattering is taken into account,[9] which implies that CaF molecules can be readily evaporatively cooled in the ultracold temperature region.

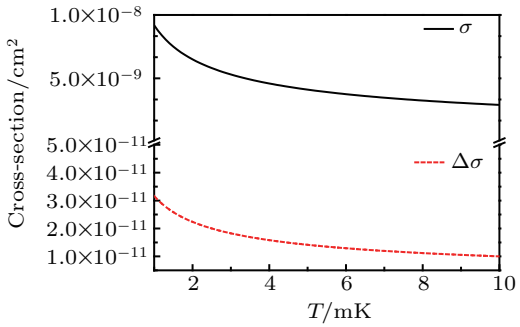


Fig. 6. The elastic cross-section σ (solid) of CaF at an orientation field of 100 kV/cm and the cross-section increment Δσ (dash) compared to σ in field-free case vs. temperature at the order of mK, when only the dipole–dipole interaction is taken into account.

In addition, Ticknor[28] pointed out that the elastic collision cross-section of the ultracold molecules in high electric field is determined by the mass, induced electric dipole, and collision kinetic energy of the collision particles, and the cross-section does not depend on the detail of the short range interaction potential until it reaches the quantum unitarity limit σ_{Q}. The temperature corresponding to the σ_{Q} of CaF is 28 nK.[28] The elastic collision cross-section σ_{SC} of CaF at the temperature of 1 μK in the field of 100 kV/cm is as high as 1.2×10^{-8} cm^2, larger than that of RbCs (3×10^{-9} cm^2) under the same condition,[28] which further implies that CaF is a good candidate to be evaporatively cooled. Furthermore, the enhancement factor of the applied field to the elastic cross-section of CaF is over 2×10^3.

Other diatomic alkaline earth fluorides were also calculated and are listed in Table 2 under the same condition. The heavier the molecule, the larger collision cross-section it has. However, this does not mean that BaF is favorable because we have to consider the cold molecular source achieved by the primary cooling method. Stark deceleration of polar molecules is one of the methods that can be used to obtain cold molecules with large molecular numbers; in which the lighter the molecule is, the easier it is slowed down. Therefore, if the cold molecular source was obtained by Stark deceleration, CaF seems to be the best candidate for further evaporative cooling to achieve a large density of ultracold molecules.

Table 2. Collision cross-sections of several diatomic radicals of alkaline earth fluorides.

Molecule	$\sigma_{\mathrm{D-D}}/10^{-9}$ cm^2	$\sigma_{\mathrm{D-ID}}/10^{-12}$ cm^2	$\sigma_{\mathrm{SC}}/10^{-8}$ cm^2
MgF	5.28	4.13	1.07
CaF	6.48	5.90	1.24
SrF	10.93	11.61	2.09
BaF	11.26	12.93	2.16

3.3. Evaporative cooling

The setup for potential evaporative cooling of cold CaF molecules is illustrated in Fig. 7. A Mach–Zehnder interferometer type optical circuit is used to form the optical trap for evaporative cooling, and the trap depth is adjusted by an acoustic-optical intensity modulator (AOM). The Gaussian laser beam is p-polarized to avoid the interfering and near-red-detuned to the transition of CaF. The simulation of the evaporative cooling followed the model developed in the group of Ketterle.[29,30] When the trapping potential decreases from $U(k_{\mathrm{B}}T)$ to $U'(\eta k_{\mathrm{B}}T)$, the molecular number N, the trapping volume V, the molecular temperature T, and the molecular density n change to N', V', T', and n', respectively. The relations are as follows:[29,30]

$$N' = N \times v^{(U-U')}, \tag{12}$$

$$V' = V \times v^{\gamma\xi(U-U')}, \tag{13}$$

$$T' = T \times v^{\gamma(U-U')}, \tag{14}$$

$$n' = n \times v^{(1-\gamma\xi)(U-U')}, \tag{15}$$

where $\xi = \frac{3}{2}$, $v = 1 - \frac{2+2\eta+\eta^2}{2\mathrm{e}^{\eta}}$, $\gamma = \frac{\log(\alpha/3v)}{\log(v)}$, and $\alpha = 3 - \frac{6+6\eta+3\eta^2+\eta^3}{2\mathrm{e}^{\eta}}$.

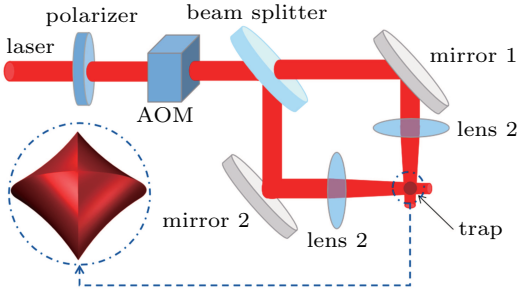


Fig. 7. All-optical, Mach–Zehnder interferometer type trap for evaporatively further cooling cold CaF molecules. The laser beam is p-polarized to avoid interfering and an AOM adjusts the laser intensity, and the trap is illustrated in three-dimensional as well.

We simulated the CaF evaporative cooling in the proposed optical trap, as shown in Fig. 7. The detuning frequency of the trapping laser was set to be 1.0 GHz red-detuned to the Q (1/2) transition (at 16493.3539 cm^{-1}) of the (0, 0) band in the A–X system of CaF, and the laser power was adjusted by the AOM from 50 mW to 12.5 mW. The adjusting sequence of the laser intensity is plotted in Fig. 8. The trap depth was decreased by 0.05 mK at each step, and the intensity kept invariant for 50 ms to wait the remained molecular cloud in the trap to re-equilibrate thermally. The cold CaF source was assumed, as demonstrated in Doyle's group,[6] to be $N = 10^5$, $V = 5.63 \times 10^{-4}$ mm^3, $T = 2$ mK, and $n = 1.78 \times 10^{11}$ cm^{-3}. Figure 9 presents the molecular parameters varying with time in the evaporative cooling procedure. The molecular loss in the cooling process is very great. This shows that when the CaF molecule is cooled to 57 μK, the molecular number will be 235 with the volume of 3.13×10^{-6} mm^3 and the density of 7.51×10^{10} cm^{-3}. The result is comparable with that of Ref. [6] despite of the lower laser power desired in the present proposal.

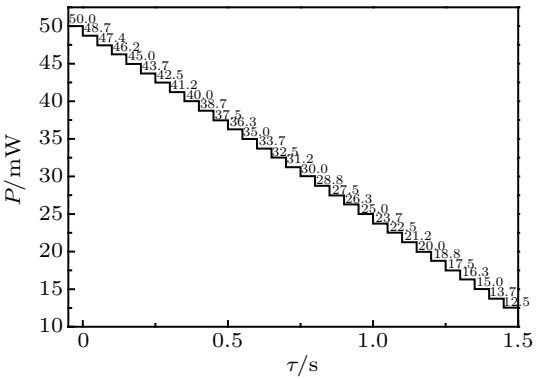


Fig. 8. The adjusting sequence of the laser power P with time τ in the evaporative cooling process.

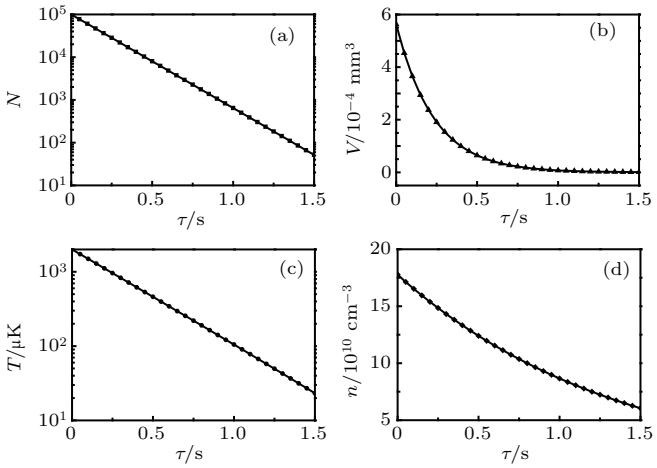


Fig. 9. (a) Molecular number N, (b) trapping volume V, (c) temperature T, and (d) molecular density n of CaF varying with time τ in the evaporative cooling procedure.

The evaporative cooling of CaF presented above represents our preliminary discussion on a potential application of our cold CaF collision study. Detailed investigations, including short/long range intermolecular interaction in the singlet/triplet states, on the evaporative cooling is currently being undertaken by our group. The more precise molecular scattering cross-section will be determined by employing the MOLSCAT[31,32] program and the cooling process will be simulated and further optimized in the all-optical trap in our next work.

4. Conclusion

The long-range dipole–dipole interaction of CaF in its ground state was investigated in the present work by employing the MOLPRO program and using the RCCSD(T)/def2-TZVP theory. High precision molecular elastic collision cross-section and collision rate were obtained. At a temperature of 2 mK, the elastic cross-section of CaF molecules is as high as 6.5×10^{-9} cm^2 and the collision rate is more than 4.1×10^6 Hz, which implies that CaF molecules are good candidates for evaporative cooling. Furthermore, the applied orientation electric field can simplify the molecular interaction potential surface function from quaternary into ternary, and can raise the collision cross-section by a factor of over 2000. Additionally, the evaporative cooling of CaF molecules (at 2 mK) in an all optical trap was discussed.

Acknowledgements

We are grateful to Dr. Liesbeth M. C. Janssen at Eindhoven University of Technology and Prof. Jeremy M. Hutson at Durham University for sending us their simulation program and their valuable discussions.

References

[1] van der Poel A P P, Zieger P C, van de Meerakker S Y T, Loreau J, van der Avoird A and Bethlem H L 2018 *Phys. Rev. Lett.* **120** 033402
[2] Stuhl B K, Hummon M T and Ye J 2014 *Annu. Rev. Phys. Chem.* **65** 501
[3] Hemmerling B, Chae E, Ravi A, Anderegg L, Drayna G K, Hutzler N R, Collopy A L, Ye J, Ketterle W and Doyle J M 2016 *J. Phys. B: At. Mol. Opt. Phys.* **49** 174001
[4] Anderegg L, Augenbraun B L, Chae E, Hemmerling B, Hutzler N R, Ravi A, Collopy A L, Ye J, Ketterle W and Doyle J M 2017 *Phys. Rev. Lett.* **119** 103201
[5] Chae E, Anderegg L, Augenbraun B L, Ravi A, Hemmerling B, Hutzler N R, Collopy A L, Ye J, Ketterle W and Doyle J M 2017 *New J. Phys.* **19** 033035
[6] Anderegg L, Augenbraun B L, Bao Y C, Burchesky S, Cheuk L W, Ketterle W and Doyle J M 2018 *Nat. Phys.* **14** 890
[7] Kajita M, Suzuki T, Odashima H, Moriwaki Y and Tachikawa M 2001 *Jpn. J. Appl. Phys.* **40** L1260
[8] Kajita M 2004 *Eur. Phys. J. D* **31** 39
[9] Kajita M 2006 *Phys. Rev. A* **74** 032710
[10] Dhont G S F, van Lenthe J H, Groenenboom G C and van der Avoird A 2005 *J. Chem. Phys.* **123** 184302
[11] Childs W J, Goodman G L and Goodman L S 1981 *J. Mol. Spectrosc.* **86** 365
[12] Werner H J, Knowles P J, Knizia G, Manby F R, *et al.* 2010 *MOLPRO* (version 2010.1, a package of *ab initio* programs)
[13] Boys S F and Bernardi F 1970 *Mol. Phys.* **19** 553

[14] Werner H J and Knowles P J 1985 *J. Chem. Phys.* **82** 5053
[15] Knowles P J and Werner H J 1985 *Chem. Phys. Lett.* **115** 259
[16] Knowles P J, Hampel C and Werner H J 2000 *J. Chem. Phys.* **112** 3106
[17] Janssen L M C, Groenenboom G C, van der Avoird A, Żuchowski P S and Podeszwa R 2009 *J. Chem. Phys.* **131** 224314
[18] Janssen L M C, Żuchowski P S, van der Avoird A and Hutson J M 2011 *J. Chem. Phys.* **134** 124309
[19] Janssen L M C, Żuchowski P S, van der Avoird A and Hutson J M 2011 *Phys. Rev. A* **83** 022713
[20] DeMille D, Glenm D R and Petricka J 2004 *Eur. Phys. J. D* **31** 375
[21] Childs W J, Goodman L S, Nielsen U and Pfeufer V 1984 *J. Chem. Phys.* **80** 2283
[22] Avdeenkov A V and Bohn J L 2001 *Phys. Rev. A* **64** 052703
[23] Fieid R W, Harris D O and Tanaka T 1975 *J. Mol. Spectrosc.* **57** 107
[24] Huang Y X, Xu S W and Yang X H 2012 *Acta. Phys. Sin.* **61** 243701 (in Chinese)
[25] Huang Y X, Xu S W and Yang X H 2013 *Chin. Phys. B* **22** 053701
[26] Sharma M K, Sharma M and Chandra S 2015 *Commun. Theor. Phys.* **64** 731
[27] Neese F 2012 *Wiley Interdiscip. Rev.: Comput. Mol. Sci.* **2** 73
[28] Ticknor C 2008 *Phys. Rev. Lett.* **100** 133202
[29] Sun H, Wang Z X, Wang Q, Li X J, Liu J P and Yin J P 2015 *Chin. Phys. B* **24** 113101
[30] Davis K B, Mewes M O and Ketterle W 1995 *Appl. Phys. B* **60** 155
[31] Hutson J M 1994 *MOLSCAT computer code,* distributed by Collaborative Computetional Project No. 6 of the Engineering and Physical Sciences Research Council (UK), version 14
[32] González-Martínez M L and Hutson J M 2007 *Phys. Rev. A* **75** 022702